Journal Pre-proofs

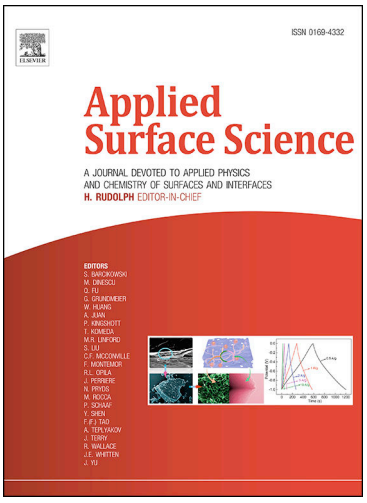

Full Length Article

Noncollinear excitation of surface plasmons for triangular structure formation on Cr surfaces by femtosecond lasers

Xin Zheng, Bo Zhao, Jianjun Yang, Yuhao Lei, Tingting Zou, Chunlei Guo

PII: S0169-4332(19)33749-3
DOI: https://doi.org/10.1016/j.apsusc.2019.144932
Reference: APSUSC 144932

To appear in: *Applied Surface Science*

Received Date: 27 June 2019
Revised Date: 1 November 2019
Accepted Date: 2 December 2019

Please cite this article as: X. Zheng, B. Zhao, J. Yang, Y. Lei, T. Zou, C. Guo, Noncollinear excitation of surface plasmons for triangular structure formation on Cr surfaces by femtosecond lasers, *Applied Surface Science* (2019), doi: https://doi.org/10.1016/j.apsusc.2019.144932

Noncollinear excitation of surface plasmons for triangular structure formation on Cr surfaces by femtosecond lasers

Xin Zheng [a,b], Bo Zhao [a,c], Jianjun Yang [a,*], Yuhao Lei [a], Tingting Zou [a,b], Chunlei Guo [a,d,*]

[a] The Guo China-US Photonics Laboratory, State Key Laboratory of Applied Optics, Changchun Institute of Optics, Fine Mechanics and Physics, Chinese Academy of Sciences, Changchun 130033, China

[b] University of Chinese Academy of Sciences, Beijing 100039, China

[c] Department of Electronic Information and Physics, Changzhi University, Changzhi, 046011, China

[d] The Institute of Optics, University of Rochester, Rochester, NY 14627, USA

* Corresponding author.

E-mail address: jjyang@ciomp.ac.cn (J. Yang)

* Corresponding author.

E-mail address: guo@optics.rochester.edu (C. Guo)

Abstract

Utilizing double time-delayed femtosecond laser pulses with different linear polarizations, we achieve the regular subwavelength triangular structure arrays on chromium surfaces in one-step processing. Both measurement and characterization reveal that such surface structures are constituted by interlocking of three ablation gratings oriented along different directions. The comprehensive investigation of the structure formation is performed by varying laser parameters such as the energy ratio, the temporal delay and the polarization discrepancy between double pulses. It is found that the ratio of double laser energies is critical for the uniform triangular structure formation especially within a temporal delay range of -10 ps < Δt <10 ps. Unexpectedly, the triangular structures can still be generated even for the double laser pulses with non-orthogonal polarizations. In theory, apart from considering the transient change of the surface optical property induced by the first laser of double pulses, we also explore the noncollinear excitation of two surface plasmons for the temporally delayed incident laser pulse, which finally results in three differently oriented grating structures. The satisfactory explanation of the experimental phenomena validates our proposed model.

Keywords: Subwavelength triangular structures; Chromium; Double femtosecond lasers.

1. Introduction

Surface micro/nano-processing technology, which is capable of controlling the surface morphology at micro/nano scales to modify the mechanical, wettability and optical properties of materials, has attracted considerable attention over the decades [1-3]. Compared with the dielectrics and semiconductors, bulk metallic materials inherently possess the high-resistance for high temperature and pressure [4-6], so that the related micro/nano-structures can perform unique superiority on some extreme environments. However, this is usually hard to carry out by the traditional lithography technologies. Recently, femtosecond laser pulses have been identified to enable producing micro/nano-structures on a variety of material surfaces in a simple and prominent way [7-11], which is so-called laser-induced periodic surface structures (LIPSS). During this technology, multiple structure units rather than the single interaction trace can be produced simultaneously within the laser beam spot, and the structure precision can be beyond the optical diffraction limit without the tight beam focusing. Other structure features such as the spatial period, the modulation depth and the distribution orientation can also be feasibly controlled by the laser parameters [12-14]. Nowadays, femtosecond LIPSSs have been employed for re-functionalization

of metal surfaces to show many valuable applications [15-18], including the enhanced optical absorber, the efficient thermal emitter, the super-hydrophobic effects, etc.

Nevertheless, the current research of the femtosecond LIPSSs is mostly concentrated on the formation of one-dimensional (1D) grating-like structures, which of course has limitations in the future application. In order to expand the simple surface structures into the complex ones, we have already fabricated two dimensional (2D) subwavelength dot-matrix structures on the bulk molybdenum surface in one step, via utilizing the temporally delayed two-color femtosecond laser pulses that are linearly polarized in orthogonal directions [19]. Moreover, through employing a birefringent crystal to generate double time delayed femtosecond laser pulses with orthogonal polarizations, we have obtained for the first time 2D periodic distribution of surface structures in both triangular and dot-matrix profiles on the bulk tungsten surfaces [20, 21]. Recently, Romano et al. reported the formation of the subwavelength triangular structures on the steel surfaces with irradiation of circularly polarized femtosecond laser pulses [22]. Similarly, Fraggelakia et al. also observed the triangular and square structures on the stainless steel surfaces through employing double time delayed femtosecond laser pulses with crossed either linear-polarization or circular-polarization, where the nonlinear convection flow of the molten materials in the nanosecond scale was proposed for the structure formation mechanism [23]. Obviously, this interpretation is not suitable for the picosecond time delays of double femtosecond pulses.

In general, the method of double-pulsed femtosecond laser irradiation provides an ideal candidate for one-step fabricating 2D periodic subwavelength structures on metals, because the transient optical properties of the metal surface induced by the first pulse can be employed for the manipulation of the interactions of the delayed second laser pulse, which eventually affects the formation process of the surface structures. However, the influence of both the laser polarization and energy on the triangular structure formation is not clear, and the deep understanding of the physical mechanisms still remains a big challenge.

In this paper, we report the one-step fabrication of the regular subwavelength triangular structures on chromium surfaces based on an interferometer-like configuration to generate double femtosecond laser pulses of picosecond time delays. First, the structure features are examined in detail by both the microscopic measurements and the Fourier domain analyses. After that, the formation of the triangular structures is experimentally controlled through varying laser parameters including the energy ratio, the temporal delay, and the polarization direction discrepancy. Moreover, a dynamic region of the structure formation is also achieved in terms of the scanning speed and the defocal distance of the sample. Finally, the deep insights into the physical origins of such structures are provided in a frame of the noncollinear excitation of the surface plasmons on the transient properties of the material surface.

2. Experimental arrangements

A schematic diagram of the experimental setup is shown in Fig. 1, where the light source is a commercial chirped-pulse-amplifier Ti: sapphire laser system (Spitfire Ace, Spectra Physics), which delivers horizontally polarized femtosecond laser pulses trains at the repetition rate of 1 kHz, with the central wavelength of 800 nm and the pulse duration of 40 fs. To generate double laser beams featured by the orthogonal polarizations and certain temporal delays, an interferometer-like optical design was introduced to split each laser pulse out of the amplifier into two identical sub-ones by a

half-reflecting mirror (HM). In one of the optical arms, a computer-controlled 1D translation stage was employed as an optical delay line to adjust the temporal delay (Δt) between the two sub-pules, and the linear polarization of the laser inside was changed by a half-wave plate. Afterwards, the laser pulses passing through two different optical paths were spatially aligned into the collinear propagation by another HR mirror, and then focused through the same objective lens (Nikon, 4×, NA = 0.13) onto a polished sample surface at normal incidence. The selection of sample material, a chromium plate with a thickness of 2 mm, was mounted on a computer-controlled three-dimensional translation stages (ESP 301, Newport) with a moving accuracy of 125 nm. In order to avoid serious ablation damages, the sample surface was moved slightly from the focal plane towards the lens. The experiments were carried out in air by translating the sample at the speeds ranging from V = 0.1mm/s to 0.4 mm/s. After the laser processing, the sample was subjected to ultrasonic cleaning in acetone for 5 min. The structural morphologies of the laser irradiated surface were characterized by scanning electron microscopy (SEM, Phenom) and atomic force microscopy (AFM, Bruker).

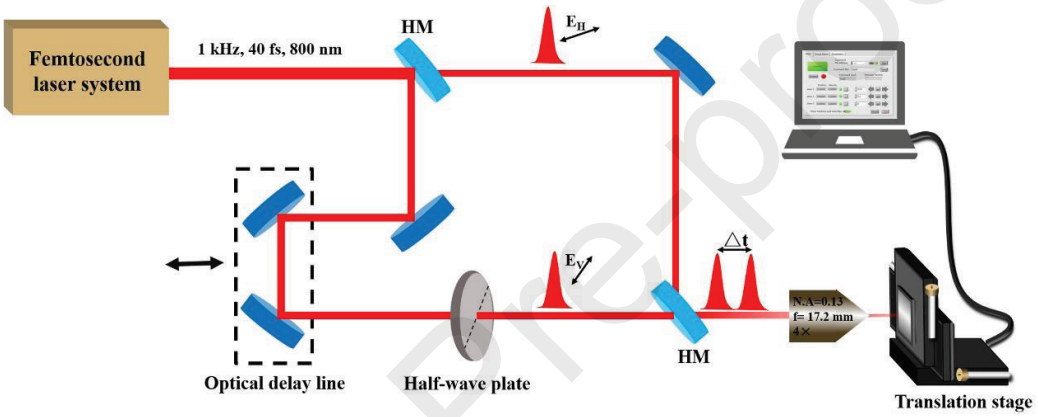

Fig. 1. Schematic diagram of the experimental setup for the formation of subwavelength triangular structures on chromium surface using orthogonally polarized double femtosecond laser pulses with certain temporal delays. HM for either splitting the laser pulse into two ones along different arms or spatial collecting the two laser pulses into a collinear propagation mode. A half-wave plate for rotating the direction of the linear polarization of one laser beam. E_H and E_V represent the electric fields of the laser pulses polarized in the horizontal and vertical directions, respectively. Optical delay line for adjusting the time delay between the two sub-pulses via a translation stage. The positive time delay indicates the first arrival of the horizontally polarized laser pulse (E_H) on the sample surface.

3. Experimental results and discussions

3.1 Structural morphology and characterization

Fig. 2 shows the obtained results on chromium surface irradiated by double femtosecond laser pulses at the inter-pulse delay of Δt = +2 ps (Note: the horizontally polarized laser pulse of E_H arrived ahead on the surface for the positive delays; whereas the vertically polarized laser pulse of E_V arrived ahead on the surface for the negative delays). Here the energy fluences of double laser pulses are identical of $F_H = F_V = 64.8$ mJ/cm^2, and the translation speed of the sample is V = 0.3 mm/s. From the SEM images of Fig. 2A, it is intuitively found that the laser-induced surface morphology is composed by 2D arrays of triangular-shaped structures at subwavelength scales, rather than the commonly observed 1D grating-like structures in many previous studies [24-27]. Or

we can say that three groups of 1D periodic grating structures begin to appear on the laser exposed surface, whose different orientations are spatially interlocked each other to construct such triangular structure arrays. The higher resolution picture suggests that each triangular structure unit is actually formed by the spatial intersection of three ablation grooves with different orientations. Interestingly, among the triangular structure arrays, one of the grating structures is evidenced to have orientation along the vertical direction, which is perpendicular (or parallel) to the polarization direction of the laser pulse E_H (or E_V), while other two grating structures are slantwise-oriented with respect to the laser polarization, i.e., their spatial orientations are neither parallel nor perpendicular to any directions of the two laser polarizations. The measured intersection angles among three grating structures approximate 60°. As a matter of fact, there exist abundant of nanoparticles deposited on the surface of the triangular structures, indicating the strong laser ablation process during the structure formation. Moreover, the measured side lengths of the triangle structure unit, as enclosed by the green solid lines, are approximately 740 ± 30 nm, and the spatial periodicities of three grating structures seem to be nearly equal to 680 ± 30 nm, being slightly smaller than the central wavelength (800 nm) of the laser. In particular, such kind of subwavelength ablation structures can be homogenously extended over a large area without breakings, bends and bifurcations, in sharp contrast to observations induced by a single beam laser irradiation [10, 11, 24, 26].

In order to qualitatively describe the topography of the aforementioned surface patterns, an AFM image of the triangular structures is obtained with the cross-section profiles along three different directions, which are marked by the black, red and green lines, respectively, as shown in Fig. 2B. It is seen that the modulation depth of the grooves acting as the boundary of the triangle unit is about 70 ± 20 nm. However, at the intersecting points of three ablation grooves, close to the triangle vertex, the modulation depth becomes as large as 230 ± 20 nm, nearly triple that of each ablation groove. From this aspect, we can understand that the laser-induced triangular structures can provide three-dimensional profiles during one-step processing, resulting in a spatially periodic modulation depth, which is much different from the plane technique of mask-based lithography [27, 28].

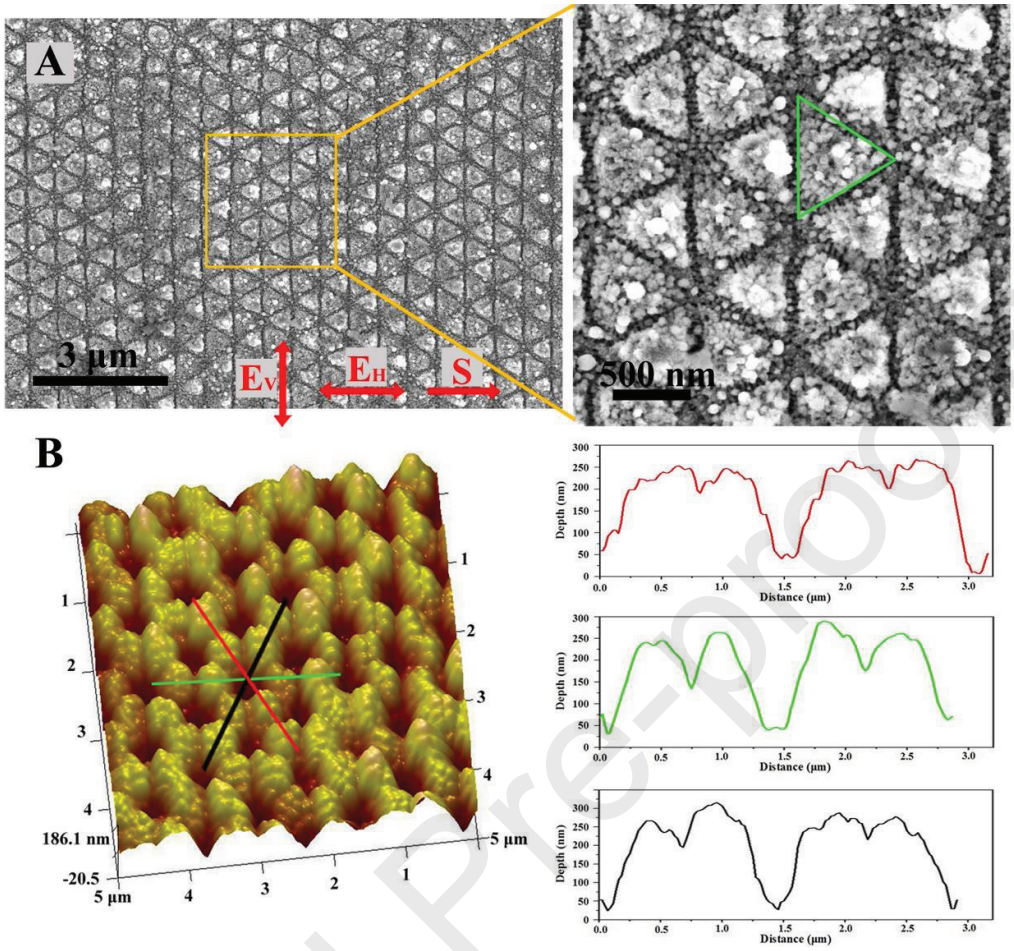

Fig. 2. The obtained subwavelength triangular structures on Cr surface under irradiation of the orthogonally polarized double femtosecond laser pulses, which have the inter-pulse delay of $\Delta t = +2$ ps and the equal energy fluence of $F_H = F_V = 64.8$ mJ/cm^2. The translation speed of the sample is set as V = 0.3 mm/s. (A) SEM images, where the double-head arrows (E_V and E_H) represent the directions of the double laser polarizations, and the single-head arrow (S) for the scanning direction; (B) An AFM image with the cross-section profiles along three different directions, as marked by the green, red and black lines.

The unique features of the aforementioned triangular surface structures were also analyzed in the frequency domain via the 2D fast Fourier transform (FFT), and the obtained results are displayed in Fig. 3A. Clearly, the achieved bright spots in the frequency domain seem to be aligned in three different directions, which are respectively perpendicular to the spatial orientations of three grating structures. This essentially confirms that the laser-induced triangular structures are in fact constituted by the spatial overlapping of three periodic gratings oriented in different directions. After performing the filtering process for the FFT image in Fig. 3A, we obtained the data only distributed in each individual directions and then re-constructed their patterns in the spatial domain through the inverse Fourier transformation, which are shown in Fig. 3B, C and D. Evidently, three individual grating-like structure distributions can be achieved. For the purpose of the convenient identification, such re-constructed patterns are named as "G_1", "G_2" and "G_3", respectively.

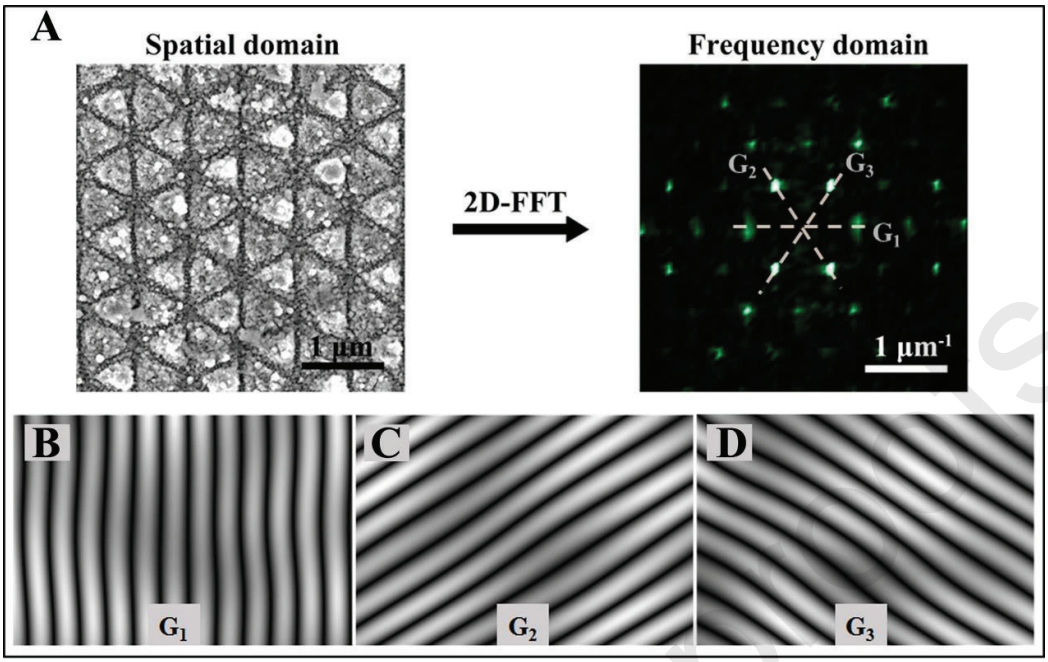

Fig. 3. (A) SEM image of the subwavelength triangular surface structures and its corresponding 2D-FFT image; (B)-(D) the spatial patterns re-constructed from the FFT data in three individual directions.

3.2 Effects of the laser parameters on the structural regularity

Based on the massive experimental data, we summarized how the triangular structure formation is affected by the large variations of laser energy ratio R of double laser pulses. As shown by the yellow region of Fig. 4A, when the laser ratio is limited within a range of $1 < R < 3$, i.e., $F_H > F_V$, the regular distribution of the subwavelength triangular structures can be generated, as shown by a bottom-right inset picture in Fig. 4A. However, when the laser ratio R decreases into a range of less than 1, i.e., $F_H < F_V$, as marked by the blue region of Fig. 4A, the formation of the triangular structures becomes deteriorated and irregular, as shown by the upper-right inset pictures in Fig. 4A. It should be noticed that the above mentioned situations only take place for the inter-pulse time delay of $-10\ ps < \Delta t < 10\ ps$, no matter which laser pulse (E_H or E_V) firstly arrives at the sample surface. Moreover, the laser energy fluences of F_H and F_V for fabrication of the triangular structures can be varied from 20 mJ/cm^2 to 140 mJ/cm^2. On the other hand, for the inter-pulse time delay $\Delta t > 10$ ps, the regular formation of the triangular structures cannot be observed even at any energy ratios. Remarkably, within the inter-pulse time delay range of $-10\ ps < \Delta t < 10\ ps$, there is always a grating component with the orientation perpendicular to the polarization direction of the larger fluenced laser pulse. For example, regardless of the sign of the inter-pulse time delay, the grating component oriented in the vertical direction (perpendicular to the laser polarization of E_H) always appears in the case of $R > 1$ ($F_H > F_V$); while the grating component oriented in the horizontal direction (perpendicular to the laser polarization of E_V) always takes place for $R < 1$ ($F_H < F_V$). These results indicate that the incident laser pulse with larger energy fluence plays an important role in the formation of the structures.

For the observed difference in the structural regularity between cases of $F_H > F_V$ and $F_H < F_V$, it can be understood by 1D LIPSS formation under irradiation of the single beam femtosecond laser

pulses with different polarization directions. As shown in Fig. 4B, for an incident femtosecond laser pulse, the resultant LIPSS is usually oriented perpendicular to its linear polarization, with somewhat distorted distribution especially near edges of the beam spot. When the sample scanning is fixed along the horizontal direction, the existed LIPSS would like to be coherently extended by the partial overlapping of multiple pulses [3, 29]. If the scanning direction is parallel (or perpendicular) to the laser polarization (or the LIPSS orientation), the new generation of LIPSSs by the subsequent pulses tends to be arranged in parallel mode, i.e., all of them exhibit the center and justify aligning in space, which eventually results in a large number of LIPSS. Under such circumstances, the distribution regularity of the structures can be maintained without adding no more distortions. On the other hand, when the scanning direction is perpendicular (or parallel) to the laser polarization (or the LIPSS orientation), the new generation of LIPSSs by the subsequent pulses becomes arranged in cascade mode, so that the longitudinal length rather than the number of the LIPSS is ready to increase. In this case the distorted situations on the terminals of the existed LIPSSs can affect the spatial alignment of the newly emerging structures, which consequently brings about the additional irregularities in the entire LIPSSs. As a matter of fact, the aforementioned analyses can be confirmed by the experimental observations in the previous studies [3, 12, 14, 25, 29]. As concerning the triangular structure formation in our experiments, the structural regularity is crucially dependent on the laser pulse of the larger energy fluence. At $R < 1$ ($F_H < F_V$), because the dominant laser pulse possesses the linear polarization of E_V, being perpendicular to the scanning direction, both its induced horizontal orientation of the grating-like structure and the finally obtained triangular patterns display the irregular appearance. While at $1 < R < 3$, ($F_H > F_V$), because the dominant laser pulse turns to have the linear polarization of E_H, which is parallel to the scanning direction, its induced vertical orientation of the grating-like structure tends to have a regular distribution, which consequently is favorable for the final formation of the uniform triangular patterns.

Fig. 5C shows SEM images of the triangular structure formation for several different inter-pulse time delays within a range of $-5\ \text{ps} \leq \Delta t \leq 5\ \text{ps}$, where the two laser fluences were given by $F_H = 42.2\ \text{mJ/cm}^2$ and $F_V = 28.4\ \text{mJ/cm}^2$, respectively. In this case, the formation of the triangle surface structures is almost undistinguishable for the same time delay values with opposite signs. Especially, the vertical orientation of the grating component is always produced despite a change of sign in the inter-pulse time delay, which indicates the predominant physical role of the laser fluence.

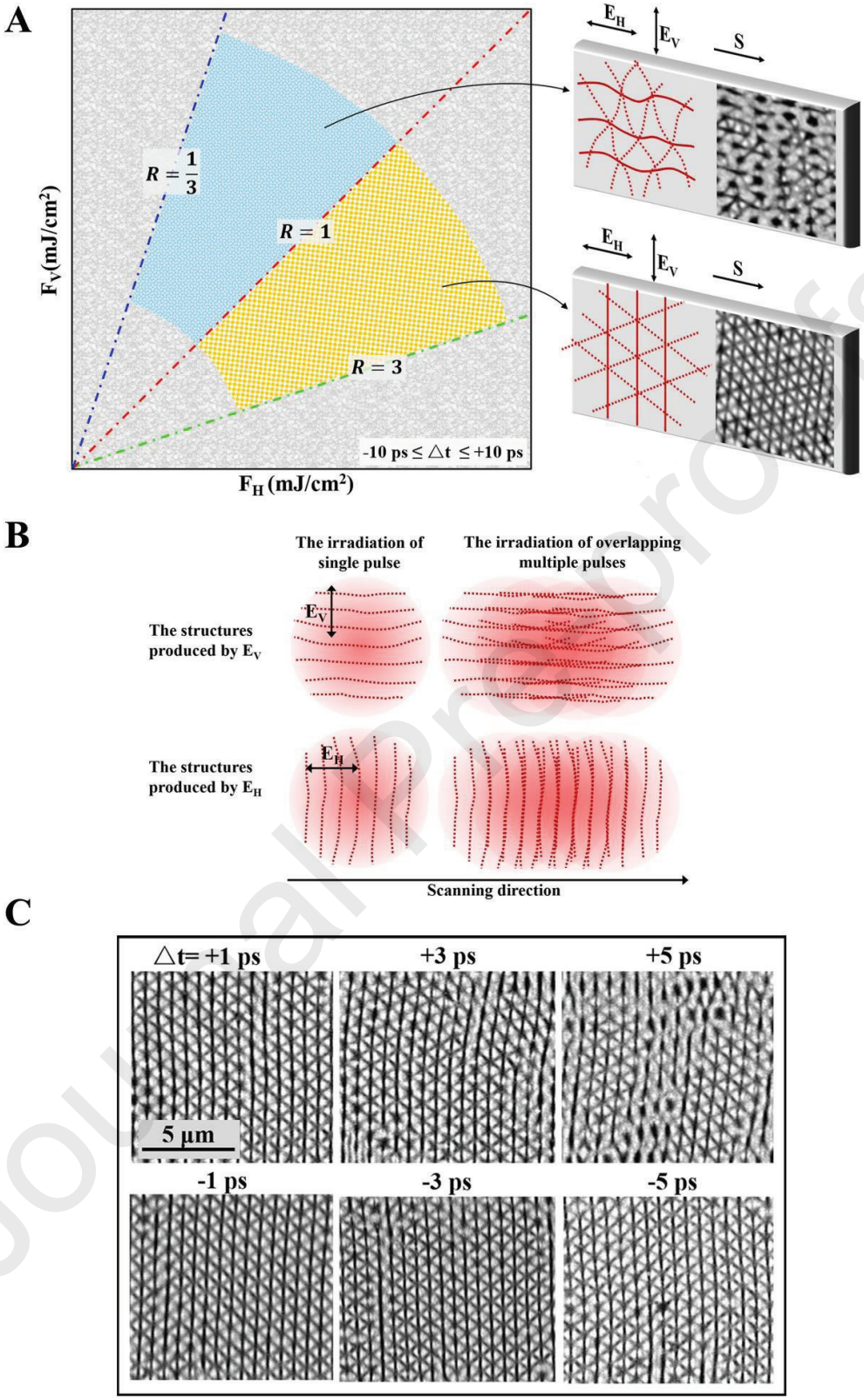

Fig. 4. (A) Measured dynamic regimes for the formation of the triangle surface structures in terms of double laser energy fluences, where R = F_H/F_V represents a ratio of two laser fluences. (B) Schematic description of the laser polarization dependent structural regularity. (C) SEM images of the triangular structures induced by double

femtosecond laser pulses at several different inter-pulse time delays of $\Delta t = \pm 1$ ps, ± 3 ps, ± 5 ps, where the double laser fluences are $F_H = 42.2$ mJ/cm^2 and $F_V = 28.4$ mJ/cm^2, respectively; and the translation speed of the sample is fixed as V = 0.3 mm/s.

3.3 Influence of the energy ratio on the structure morphology

In the experiment, we also investigated the morphological evolution of the triangular surface structures with increasing the energy ratio of $R = F_H/F_V$, and the results are illustrated in Fig. 5. In general, for the given translation speed of V = 0.3 mm/s and the inter-pulse time delay of $\Delta t = +2$ ps, the morphology of the triangular structures does not exhibit the remarkable differences at different energy ratios, among which F_H value is gradually increased when $F_V = 57.9$ mJ/cm^2. This indicates the formation of such structures is robust in some degree against the fluctuations of the laser energy fluence. For the three grating structures involved, the measured variations in both the spatial periodicities and the ablation depths versus the energy ratio are shown in Fig. 5B and C, respectively. It is seen that three grating periodicities slightly decrease with increasing the laser energy ratio, but the periodicity of the G_1 (oriented in the vertical direction) seems to be always smaller than those of other two gratings. The modulation depth of three grating structures becomes shallower as the laser energy ratio increases, which can be attributed to the weakening of the electron-phonon coupling with increasing electron temperature caused by the larger laser energy [26, 30].

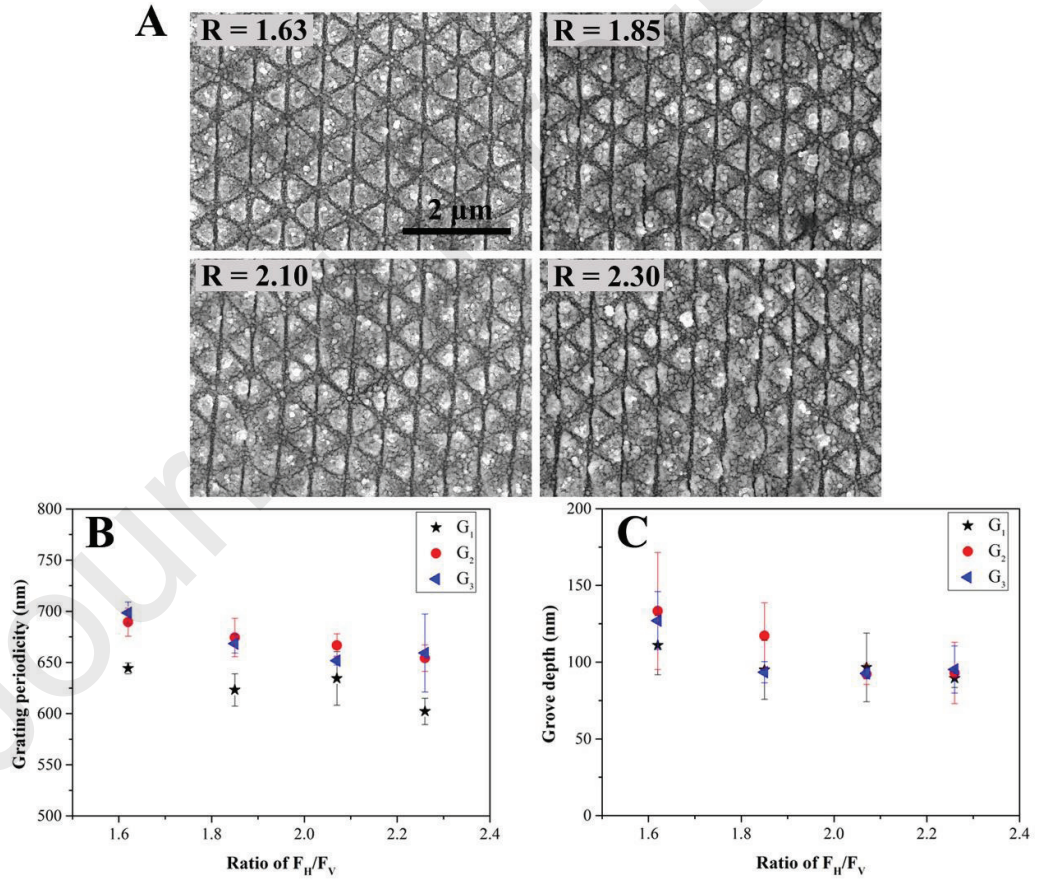

Fig. 5. Formation of the triangular surface structures with different ratios of double laser energy fluences. (A) SEM images of the triangular structures at different laser energy ratios of R = 1.63, 1.85, 2.1 and 2.3. Measured periodicities (B) and modulation depths (C) of the grating structures as a function of the laser energy ratio.

3.4 Dependence of the double laser polarizations

Meanwhile, the effects of the laser polarizations on the triangular structure formation are experimentally investigated as well. As shown in Fig. 6, when the inter-pulse time delay is given by $\Delta t = +2$ ps apart from the orthogonally polarized situation, the triangular surface structures can still be achieved even for the double laser pulses with other crossed polarizations, i.e., the intersection angle (α) between directions of the two laser polarizations with other different values such as 80°, 60° and 40°, which is obtained by rotating the polarization direction of the second laser pulse (E_V) under maintaining the horizontal polarization of the first laser pulse (E_H). Obviously, with smaller intersection angles of α, the triangular structures can still be generated on the sample surface but become progressively less regular, along with the clockwise change in orientation of the ablation grooves. This indicates the polarization effects of the second laser pulse on the triangular structure orientation. For instance, as the intersection angle decreases from $\alpha = 90^o$ to 80^o, the change degree of the structure orientation is approximately 5^o; when α value is reduced from 80° to 60°, the structure orientation has a rotation degree of about 6^o. Except for the case of $\alpha = 90°$, the resultant three grating orientations are neither parallel nor perpendicular to any directions of the laser polarization. Especially when $\alpha \leq 40°$, the triangular structure formation disappears and it is replaced by the irregular distribution of 1D semi-periodic grating structures.

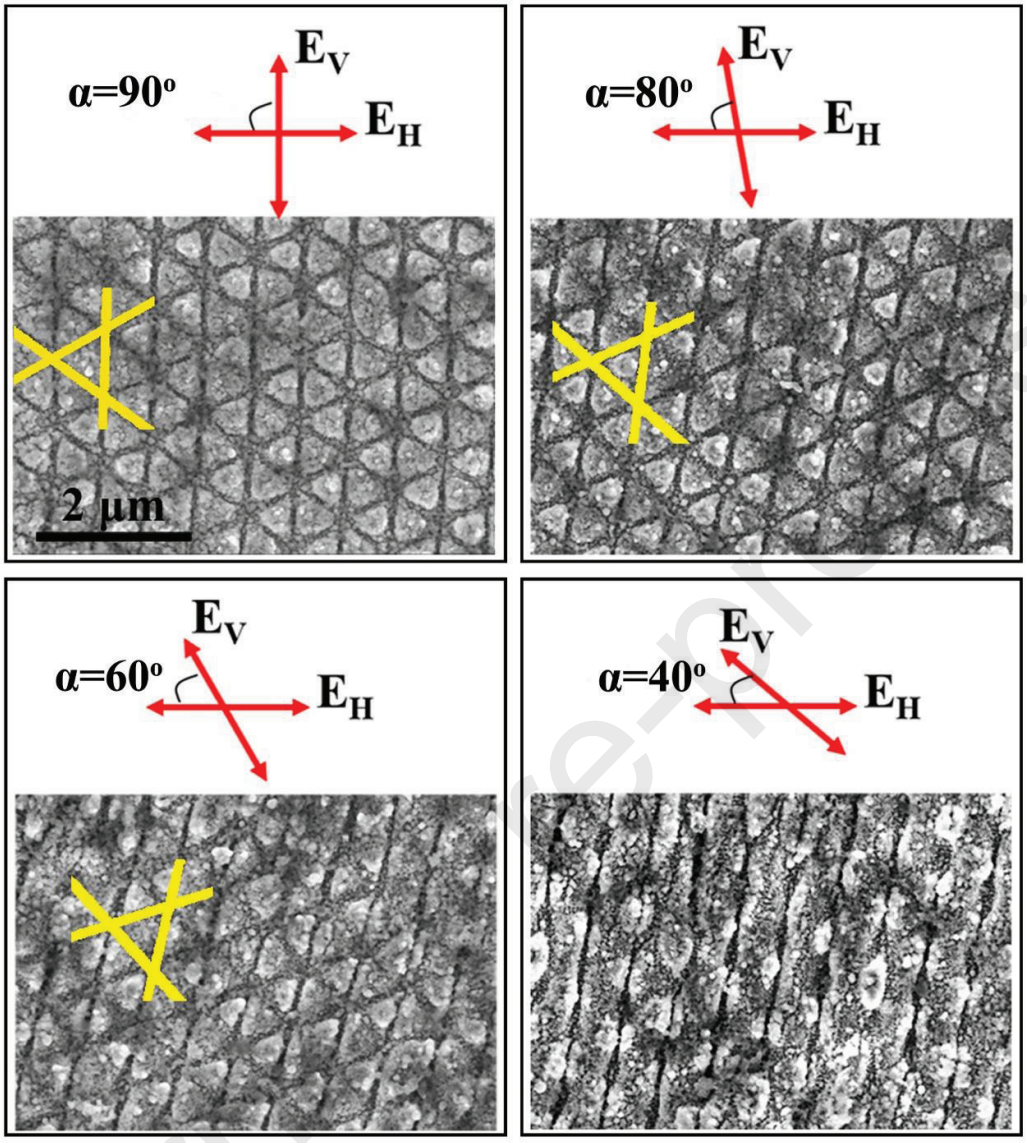

Fig. 6. Variations of the surface structures under irradiation of double laser pulses with different intersection angles between their polarization directions, such as α = 80°, 60° and 40° (F_H = 78.3 mJ/cm^2, F_V = 57.7 mJ/cm^2, V= 0.2 mm/s).

3.5 Dynamic region for the structure formation

In order to survey the influence of other laser parameters on the triangular structure formation, we repeated the experiment with varying the scanning speed and the defocal distance of the sample at the fixed laser energy ratio of R = 1.412. As shown by the statistical data in Fig. 7A, the laser-induced triangular structures usually take place in the region shadowed by the yellow color. From its inverted trapezoidal outline profile, we can find that the dynamic range of the suitable scanning speed becomes increased at larger defocal distances. On contrary, if the laser parameters are out of this processing window, the obtained surface structures tend to display 1D grating patterns, similar to the common observations induced by the single beam femtosecond laser irradiation [10, 12]. For example, when the defocal distance was less than 300 μm, which corresponds to the higher laser

fluence, the formation of the triangular structures never happens whatever the scanning speed becomes. Now we conclude that the induced triangular structures are not only dependent on the laser energy ratio, but also closely related to the absolute energy fluence and the number of the laser pulses. Finally, on the basis of our achieved window conditions for the triangular structures, we fabricated the regular triangular structures on a large area of the Cr surface, as shown in Fig. 7B. Remarkably, such subwavelength triangular structures can be substantially extended into the entire surface of Cr plate.

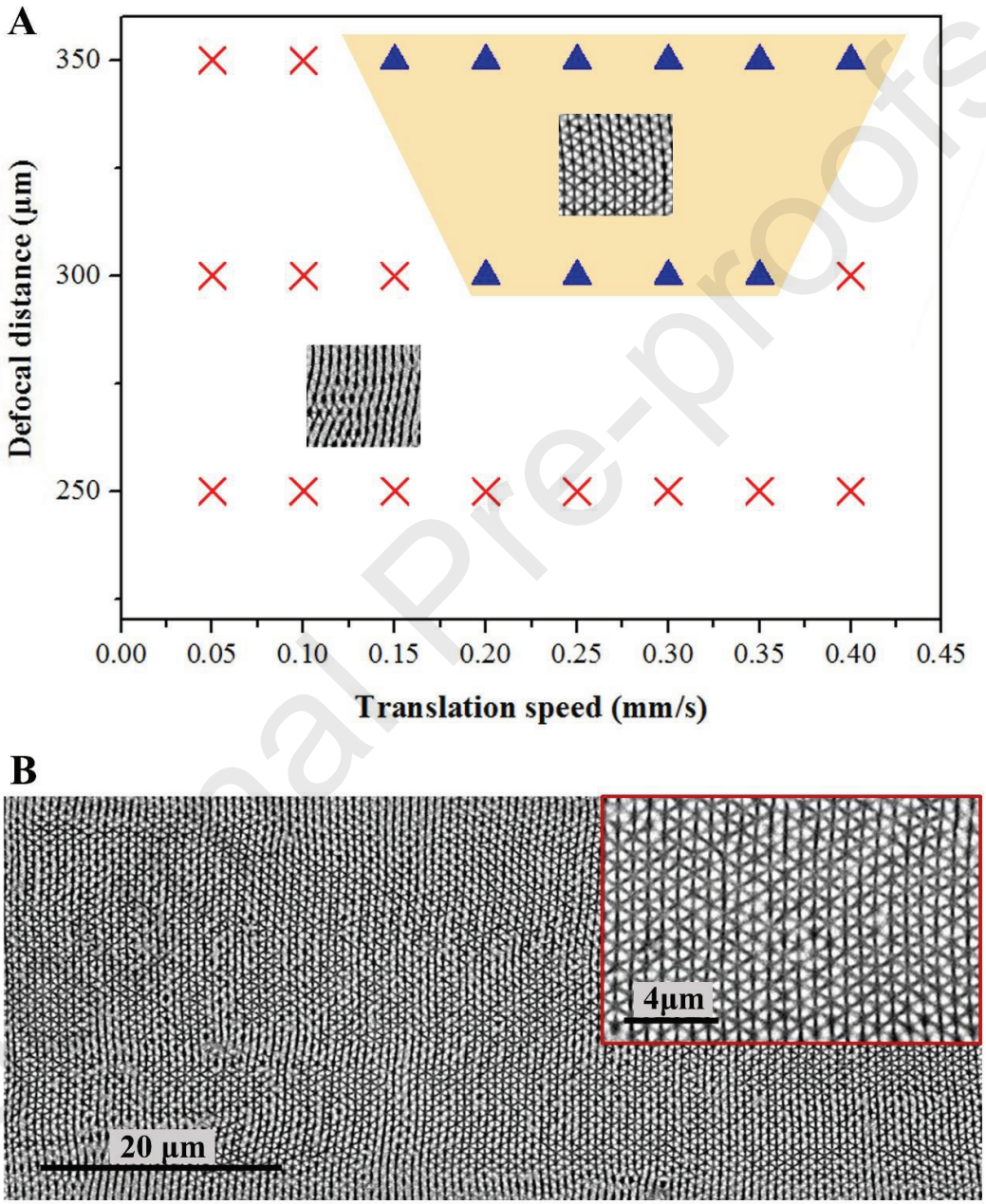

Fig. 7. (A) Experimentally obtained window conditions for fabricating surface structures in terms of both the defocal distances and the translation speeds of the sample at the laser energy ratio of R = 1.412, where the inset SEM images respectively show the structural morphologies represented by the symbols of '▲' and '×'. (B) The obtained large-area regular triangular structures at the laser fluence of F_H = 102.38 mJ/cm^2 and F_V = 72.2 mJ/cm^2, with the translation

speed of V = 0.25 mm/s and inter-pulse time delay of Δt = 2 ps.

3.6 Exploration of the underlying mechanisms

The relevant physical processes for the formation of the triangular surface structures can be depicted as follows: During the irradiation of double pulses, the firstly incident femtosecond laser pulse is able to introduce the spatially subwavelength periodic modulation on the optical properties of the sample surface, through the emergence and action of the intensity fringes originated from the interference of the laser with the excitation of surface plasmon polaritons (SPP) [22, 26]. Such behaviors consequently result in the so-called transient refractive index grating (TRIG) patterns on the material surface especially within the energy relaxation process [4, 21, 30], where the grating orientation is perpendicular to the direction of the linear polarization of the first laser pulse, very similar to the situations of a single-beam laser irradiation. When the secondly (or temporally delayed) incident femtosecond laser pulse arrives only after picoseconds of time delay, its energy coupling with the material surface is expected to be changed because of the still existence of the TRIG.

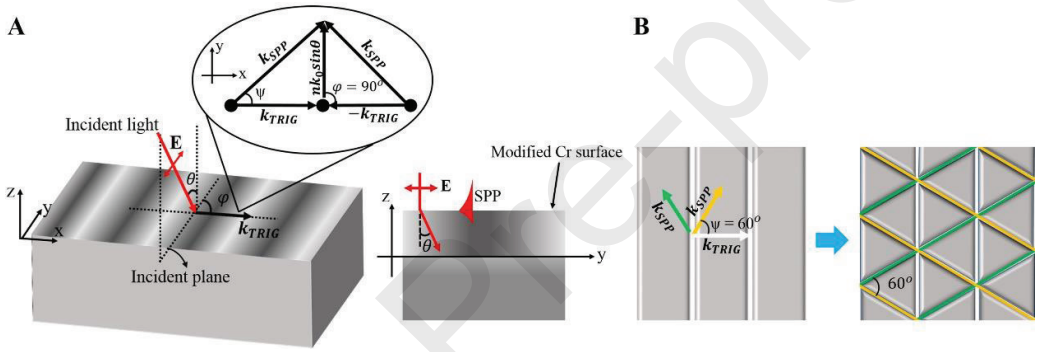

Fig. 8. Proposed model for the femtosecond laser-induced triangle structure formation on the metal surface. (a) Noncollinear excitation of SPPs on the modified surface layer with a transient refractive index grating (TRIG), where the upper-right insert is a 2D reciprocal space representation of two SPPs generation at the condition of $\theta \neq 0$ and $\varphi = 90^{o}$. $\mathbf{nk_0 sin\theta}$ and $\mathbf{k_{TRIG}}$ represent the wave and grating vector for the incident laser and TRIG, respectively. The right image indicates the light deflection behavior when passing through the laser modified surface layer of the material. **E** represents the electric field of the incident TM polarized light. (b) The simultaneous generation of two SPPs propagating along different directions on the TRIG surface (left), and the formation of the triangular structures is originated from the spatial interlocking among three ablation gratings induced by two $\mathbf{k_{SPP}}$ and $\mathbf{k_{TRIG}}$ (right).

Due to the double laser pulses having orthogonal polarization state, the electric field direction of the second laser pulse is in fact parallel to the spatial orientation of the TRIG induced by the first laser pulse. According to the analyses of Ref. [31], under such circumstances if the incident light is TE polarized there is no excitation of SPP for the incident light with TE polarization. However, when the incident light is considered as TM polarization, as Fig. 8A shown, where the azimuth angle φ of the incident plane with respect to the transient grating vector is 90^{o} and the incident angle θ is not zero, two SPPs can be excited simultaneously by scattering from the grating vector $\pm \mathbf{k_{TRIG}}$. And their relationship should follow the phase matching conditions

$$\mathbf{k_{SPP}} = \mathbf{nk_0 sin\theta} \pm \mathbf{k_{TRIG}} \quad (\theta \neq 0) \qquad (1)$$

where, $\mathbf{nk_0 sin\theta}$ represents the effective wave vector of the incident light on the target surface for exciting of SPP modes (n is the refractive index of the surrounding dielectric material). $\mathbf{k_{SPP}}$

represents the wave vector of the excited SPPs. Because the directions of $\mathbf{k_{TRIG}}$ and $\mathbf{nk_0 sin\theta}$ have a noncollinear scheme, the excitation of SPPs can be calculated in noncollinear geometry, as indicated by the upper-right inset in Fig. 8A. Therefore, the propagation directions of two $\mathbf{k_{SPP}}$ with respect to $\mathbf{k_{TRIG}}$ can be described by an angle ψ, i.e.,

$$\psi = \sin^{-1}(nk_0 \sin\theta / k_{SPP}) = \sin^{-1}(n\sin\theta \lambda_{SPP}/\lambda_0) \quad (2)$$

where λ_{SPP} and λ_0 represent the wavelengths of the laser and the excited SPPs, respectively. As shown in Fig. 8B, the two excited SPP waves will subsequently generate two groups of the intensity fringes, which finally result in two differently oriented grating structures through energy deposition and material ablation processes. In addition, when the ablation periodic structure from the TRIG pattern induced by the firstly incident laser pulse is also taken into account, three groups of ablation grating structures with different orientations are formed, leading to the two dimensional periodic arrays of triangular-shaped subwavelength structures on the laser-exposed surface. Because our measured intersection angles among the three groups of ablation gratings forming the triangular structures was $\psi = 60^o$ the value of θ can be calculated by

$$n\sin\theta = \sqrt{3}/2 \times \lambda_0/\lambda_{SPP} = 0.51 \quad (3)$$

where $\lambda_{SPP} = 2\lambda_{TRIG}$ ($\lambda_{TRIG} = 680$ nm is the period of TRIG) and $\lambda_0 = 800$ nm.

It should be noted that during our practical experiments, the time-delayed pulse with TM polarization arrived onto the TRIG surface at the normal incidence, i.e. $\theta = 0^o$, and it seems to be unable to support the SPP excitation. However, under the condition of double femtosecond laser irradiation, the incidence of the first laser pulse is ready to modify the optical properties within a thin layer of the metal surface within the irradiation spot [32], whose refractive index exhibits a spatially gradient variation with the maxima in the center of laser irradiation spot due to the Gaussian laser beam profile, as shown by the right picture in Fig. 8A. Therefore, the optically modified thin layer surface is equivalent to a convex lens, which makes the incidence of time-delayed laser pulse become deviated, with a deflection angle of θ [33]. Of course, such behaviors can help to result in the SPP excitation on the interface between the modified surface layer and the surrounding air substance [34]. If the refractive index of the thin layer surface is supposed to have a slight modification into be n = 3 (the tabulated value is $n_{Cr} = 3.16$), we can obtain the deflected angle of $\theta = \sin^{-1}(0.51/n) \approx 9.8^o$, which sounds reasonable and can be properly adopted in the calculations. Based on the above analyses, we can understand that the most important factors for generating the triangular surface structures are $\theta \neq 0$ and $\varphi = 90^o$, both of which are very necessary to simultaneously excite two SPPs along different directions.

On the other hand, for the case of negative time delays (Fig. 5C), the observed vertically aligned grating structure can be attributed to the result of SPP excitation of the delayed incident laser pulse during the early stage double-pulse accumulation process, because the TRIG patterns induced by the first pulse (E_V) are easily smeared out by the interaction of the second laser pulse (E_H) with larger energy fluence [14]. Consequently, during the next double-pulse irradiation after the time interval of 1ms (which corresponds to the laser repetition rate of 1kHz), the existence of the precursor grating patterns tend to improve the optical absorption of the first laser pulse (E_V), which causes the sufficient modification of the material surface to deflect the laser incidence. Once the condition of $\theta \neq 0$ is satisfied, both SPP waves can be excited simultaneously. For the irradiation of delayed laser pulse (E_H), however, its SPP excitation takes place along the grating vector of the precursor grating structure because of the horizontal polarization, which can only help to enhance the formation of the already existed precursor grating structure. In other words, during these

processes there are still three groups of the gratings that can be generated, which leads to the formation of the triangular structures.

For the larger positive inter-pulse time delays, i.e., $\Delta t > +10$ ps, the TRIG patterns induced by the first incident laser pulse (E_H) begin to attenuate and even diminished because of the lattice thermal diffusion effect, [30]. Therefore, the SPP excitation of the secondly incident laser pulse (E_V) is weakened, which makes the triangular structure become irregular and finally replaced by 1D periodic grating structures. On the other hand, for $\Delta t < -10$ ps, the modified thin layer of the material surface by the first laser pulse (E_V) becomes weakened and even disappear, so that the SPP excitation of the delayed incident laser pulse (E_H) are not supported. Finally, the regular triangular structures cannot be formed. Furthermore, when directions of double laser have other intersecting angles such as $\alpha = 40^o$, 60^o and 80^o, the time-delayed laser irradiation can be considered to have an incident plane of TM component, with the azimuth angle of $\varphi = 90^o$, which can be used for exciting two SPPs simultaneously. Because the laser intensity of TM component depends on the intersection angle between the two laser polarizations, the triangular structures may be not generated at the smaller values of the intersection angle α. Such kind of expectation is consistent with the experimental observations (Fig. 6).

4 Conclusions

In summary, we have reported an efficient one-step approach to fabricate 2D periodic arrays of the subwavelength triangular structures on the bulk chromium surface under irradiation of double temporally delayed femtosecond laser pulses with different linear polarizations. The structure morphologies have been characterized by the high-resolution SEM and AFM images and analyzed in the frequency domain via fast Fourier transform, and their consisting of three grating-like components with the spatial interlocking have provided the evidence for the noncollinear plasmonic nano-printing of double femtosecond lasers. The measured spatial periodicities and the modulation depths of three grating structures are approximately 680 ± 30 nm and 70 ± 20 nm, respectively. In order to have a comprehensive study and control of the structure formation, we have repeated the experiment with variable laser parameters. It has been found that the non-degenerate configuration of the two laser polarization directions is very necessary for the triangular morphology, whose intersection angle should be large than 60^o. For the generation of triangular surface structures, the inter-pulse time delay should be less than ±10 ps, and the energy ratio of the double laser pulses is required to locate within the range of $1 < R < 3$. If the energy ratio is varied to the range of $1/3 < R < 1$, the triangular structures can still be observed but with the worse spatial distribution. The dependencies of the structure regularity and the periodicity on the energy ratio has been also analyzed.

On the other hand, for a given energy ratio, the triangle structure formation has been found to depend on both the defocal distance and the scanning speed of the sample, and the processing window has been successfully established with the statistical data of the experiment, during which the suitable scanning speed for the triangular structures becomes increased at larger defocal distances. Otherwise, the laser-induced surface morphology tends to show the traditional 1D grating-like patterns. Finally, we have tried to explore the formation mechanisms of the triangular structures by reasonable considering the transient property change of the sample surface during double laser irradiation, wherein the first laser pulse would like to induce the transient refractive

index grating on the surface, and its coupling with the second laser pulse can result in two excited surface plasmons propagating in different directions. Of course, the noncollinear excitation of two surface plasmons requires the two laser pulses to have orthogonal polarizations (or components). Therefore, three sets of the ablation gratings are eventually obtained and their spatial interlocking can result in the triangular structure profiles. The triangular structures shown in this paper have a great potential applications in the fields of optical nano-antennas, surface enhanced Raman epectroscopy and plasmonic sensors [35-37]. Moreover, the presented methodology will be expected helpful in high-speed fabrication of 2D complex subwavelength structures and to support the development of micro/nano-photonics devices.

Acknowledgements

The authors would like to acknowledge the support from National Natural Science Foundation of China (91750205, 11674178), Jilin Provincial Science & Technology Development Project (20180414019GH), Natural Science Foundation of Tianjin City (17JCZDJC37900), and K. C. Wong Education Foundation (GJTD-2018-08).

References

[1] A. Y. Vorobyev, C. Guo, Direct femtosecond laser surface nano/microstructuring and its applications, Laser Photonics Rev. 7 (2012) 1-23, https://doi.org/10.1002/lpor.201200017.

[2] W. L. Barnes, A. Dereux, T. W. Ebbesen, Surface plasmon subwavelength optics, Nature 424 (2003) 824–830, https://doi.org/10.1038/nature01937.

[3] L. Wang, Q. Chen, X. Cao, R. Buividas, X. Wang, S. Juodkazis, H. Sun, Plasmonic nano-printing: large-area nanoscale energy deposition for efficient surface texturing, Light Sci. Appl. 6 (2017) e17112, https://doi.org/10.1038/lsa.2017.112.

[4] H. Sai, Y. Kanamori, H. Yugami, High-temperature resistive surface grating for spectral control of thermal radiation, Appl. Phys. Lett. 82 (2003) 1685–1687, https://doi.org/10.1063/1.1560867.

[5] L. A. Ibbotson, A. Demetriadou, S. Croxall, O. Hess, J. J. Baumberg, Optical nano-woodpiles: large-area metallic photonic crystals and metamaterials, Sci. Rep. 5 (2015) 8313, https://doi.org/10.1038/srep08313.

[6] V. Rinnerbauer, S. Ndao, Y. X. Yeng, J. J. Senkevich, K. F. Jensen, J. D. Joannopoulos, M. Soljacic, I. Celanovic, R. D. Geil, Large-area fabrication of high aspect ratio tantalum photonic crystals for high-temperature selective emitters, J. Vac. Sci. Technol. B 31(2013) 011802, https://doi.org/10.1116/1.4771901.

[7] H. Qiao, J. Yang, F. Wang, Y. Yang, J. Sun, Femtosecond laser direct writing of large-area two-dimensional metallic photonic crystal structures on tungsten surfaces, Opt. Exp. 23 (2007) 26617–26627, https://doi.org/10.1364/OE.23.026617.

[8] M. Huang, F. Zhao, Y. Cheng, N. Xu, Z. Xu, Origin of laser-induced near-subwavelength ripples: interference between surface plasmons and incident laser, ACS Nano 3 (2009) 4062–4070, https://doi.org/10.1021/nn900654v.

[9] J. Wang, C. Guo, Formation of extraordinarily uniform periodic structures on metals induced by femtosecond laser pulses, J. Appl. Phys. 100 (2006) 023511, https://doi.org/10.1063/1.2214464.

[10] H. M. V. Driel, J. E. Sipe, J. F. Young, Laser-induced periodic surface structure on solids: a universal phenomenon, Phys. Rev. Lett. 49 (1982) 1955–1958, https://doi.org/10.1103/PhysRevLett.49.1955.

[11] A. Borowiec, H. K. Haugen, Subwavelength ripple formation on the surfaces of compound semiconductors irradiated with femtosecond laser pulses, Appl. Phys. Lett. 82 (2003) 4462–4464,

https://doi.org/10.1063/1.1586457.

[12] A. Y. Vorobyev, C. Guo, Femtosecond laser-induced periodic surface structure formation on tungsten, J. Appl. Phys. 104 (2008) 063523, https://doi.org/10.1063/1.2981072.

[13] T. Wang, C. Guo, Angular effects of nanostructure-covered femtosecond laser induced periodic surface structures on metals, J. Appl. Phys. 108 (2010) 073523, https://doi.org/10.1063/1.3487934.

[14] Y. Yang, J. Yang, L. Xue, Y. Guo, Surface patterning on periodicity of femtosecond laser-induced ripples, Appl. Phys. Lett. 97 (2010) 141101, https://doi.org/10.1063/1.3495785.

[15] A. Y. Vorobyev, V. S. Makin, C. Guo, Brighter light sources from black metal: significant increase in emission efficiency of incandescent light sources, Phys. Rev. Lett. 102 (2009) 234301, https://doi.org/10.1103/PhysRevLett.102.234301.

[16] J. Yang, Y. Yang, B. Zhao, Y. Wang, X. Zhu, Femtosecond laser-induced surface structures to significantly improve the thermal emission of light from metals, Appl. Phys B. 106 (2012) 349–355, https://doi.org/10.1007/s00340-011-4834-3.

[17] A. Y. Vorobyev, T. Y. Hwang, C. Guo, Enhanced efficiency of solar-driven thermoelectric generator with femtosecond laser-textured metals, Opt. Exp. 19 (2011) A824-A829, https://doi.org/10.1364/OE.19.00A824.

[18] A. Y. Vorobyev, C. Guo, Colorizing metals with femtosecond laser pulses, Appl. Phys. Lett. 92 (2008) 041914, https://doi.org/10.1063/1.2834902.

[19] J. Cong, J. Yang, B. Zhao, X. Xu, Fabricating subwavelength dot-matrix surface structures of Molybdenum by transient correlated actions of two-color femtosecond laser beams, Opt. Exp. 4 (2015) 5357-5367, https://doi.org/10.1364/OE.23.005357.

[20] H. Qiao, J. Yang, J, Li, Q, Liu, J, Liu, C. Guo, Formation of subwavelength periodic triangular arrays on tungsten through double-pulsed femtosecond laser irradiation, Materials 11 (2018) 2380, https://doi.org/10.3390/ma11122380.

[21] Q. Liu, N. Zhang, J. Yang, H. Q, C. Guo, Direct fabricating large-area nanotriangle structure arrays on tungsten surface by nonlinear lithography of two femtosecond laser beams, Opt. Exp. 26 (2018) 11718-11727, https://doi.org/10.1364/OE.26.011718.

[22] J-M. Romano, A. Garcia-Giron, P. Penchev, S. Dimov, Triangular laser-induced submicron textures for functionalising stainless steel surfaces, Appl. Surf. Sci. 440 (2018) 162–169, https://doi.org/10.1016/j.apsusc.2018.01.086.

[23] F. Fraggelakisa, G. Mincuzzia, J. Lopez, I. Manek-Hönninger, R. Kling, Controlling 2D laser nano structuring over large area with double femtosecond pulses, Appl. Surf. Sci. 470 (2019) 677–686, https://doi.org/10.1016/j.apsusc.2018.11.106.

[24] J. Bonse, A. Rosenfeld, J. Krger, On the role of surface plasmon polaritons in the formation of laser-induced periodic surface structures upon irradiation of silicon by femtosecond laser pulses, J. Appl. Phys. 106 (2009) 104910, https://doi.org/10.1063/1.3261734.

[25] Y. Lei, N. Zhang, J. Yang, C. Guo, Femtosecond laser eraser for controllable removing periodic microstructures on Fe-based metallic glass surfaces, Opt. Exp. 26 (2018) 5102-5110, https://doi.org/10.1364/OE.26.005102.

[26] G. D. Tsibidis, E. Skoulas, E. Stratakis, Ripple formation on Nickel irradiated with radially polarized femtosecond beams, Opt. Lett. 4 (2015) 5172-5175, https://doi.org/10.1364/OL.40.005172.

[27] X. Luo, T. Ishihara, Subwavelength photolithography based on surface-plasmon polariton resonance, Opt. Exp. 12 (2004) 3055-3065, https://doi.org/10.1364/OPEX.12.003055.

[28] Z. Tang, A. Wei, Fabrication of anisotropic metal nanostructures using innovations in template-assisted lithography, ACS NANO 6 (2012) 998-1003, https://doi.org/10.1021/nn300375r.

[29] B. Öktem, I. Pavlov, S. Ilday, H. Kalaycıoğlu, A. Rybak, S. Yavaş, M. Erdoğan, F. Ö. Ilday, Nonlinear laser

lithography for indefinitely large-area nanostructuring with femtosecond pulses, Nature Photonics 7 (2013) 897-901, https://doi.org/10.1038/nphoton.2013.272.

[30] J. P. Colombier, F. Garrelie, N. Faure, S. Reynaud, M. Bounhalli, E. Audouard, R. Stoian, F. Pigeon, Effects of electron-phonon coupling and electron diffusion on ripples growth on ultrafast-laser-irradiated metals, J. Appl. Phys. 111 (2012) 024902, https://doi.org/10.1063/1.3676221.

[31] Z. Chen, Grating coupled surface plasmons in metallic structures, University of Exeter, 2007, pp. 45-71.

[32] S. Sakabe, M. Hashida, S. Tokita, S. Namba, K. Okamuro, Mechanism for self-formation of periodic grating structures on a metal surface by a femtosecond laser pulse, Phys. Rev. B 79 (2009) 033409, https://doi.org/10.1103/PhysRevB.79.033409.

[33] C. Sheng, H. Liu, S. Zhu, D. A. Genov, Active control of electromagnetic radiation through an enhanced thermo-optic effect, Sci. Rep. 5 (2015) 8835, https://doi.org/10.1038/srep08835.

[34] C. Zhong, K. E. Ballantine, C. Kervick, C. M. Smith, D. Mullarkey, I. V. Shvets, J. F. Donegan, D. McCloskey, Mapping of surface plasmon dispersion in thin Ag–Au layered composite films, Journal of the Optical Society of America B 33 (2016) 566-573, https://doi.org/10.1364/JOSAB.33.000566.

[35] B. Roxworthy, K. Ko, A. Kumar, K. Fung, E. Chow, G. Liu, N. Fang, K. Toussaint, Application of plasmonic bowtie nanoantenna arrays for optical trapping, stacking, and sorting, Nano. Lett. 12 (2012) 796–801, https://doi.org/10.1021/nl203811q.

[36] F. Peyskens, A. Dhakal, P. Dorpe, N. Thomas, R. Baets, Surface enhanced raman spectroscopy using a single mode nanophotonic-plasmonic platform, ACS Photonics 3 (2016) 102−108, https://doi.org/10.1021/acsphotonics.5b00487.

[37] N. Liu, M. Tang, M. Hentschel, H. Giessen, A. Alivisatos, Nanoantenna-enhanced gas sensing in a single tailored nanofocus, Nat. mat. 10(2011) 631-636, https://doi.org/10.1038/nmat3029.

Xin Zheng: Investigation, Data Curation, Writing. Bo Zhao: Reviewing and Editing. Yuhao Lei: Original draft preparation. Tingting Zou: Original draft preparation. Jianjun Yang: Supervision and Reviewing. Chunlei Guo: Supervision and Reviewing.

Declaration of interests

☒ The authors declare that they have no known competing financial interests or personal relationships that could have appeared to influence the work reported in this paper.

☐The authors declare the following financial interests/personal relationships which may be considered as potential competing interests:

- Highly regular distribution of the subwavelength triangular structures on Cr surface is formed using double time-delayed femtosecond laser pulses.
- The dependence of the structure formation on the energy ratio, polarization deviation and time delay of double laser pulses are investigated comprehensively.
- The dynamic region for the formation of the regular triangular structures is presented.
- The physical contribution of the noncollinear excitation of surface plasmons to the triangular structure formation is clarified.